Indian Geotechnical Journal, 35 (4), 2005

Pseudo-Static Analysis of Nailed Vertical Excavations in Sands

Swami Saran*, Satyendra Mittal† and Meenal Gosavi‡

Introduction

Soil nailing is a method of reinforcing the soil with steel bars or other materials. The purpose is to support the tensile and shear stresses in soil and restrain its lateral displacements. The nails are either placed in drilled bore holes and grouted along their total length to form, 'grouted nails', or simply driven into the ground as 'driven nails'. The technique permits stabilization of both natural slopes and vertical or inclined excavations.

Many investigators (Stocker et al., 1979; Shen et al., 1981; Schlosser, 1982; Elias and Juran, 1989; Juran and Elias, 1990; Bridle and Barr, 1990; Ramlingaraju, 1996; Gupta, 2003) have proposed methods for investigating the stability of vertical / nearly vertical excavations. In each method, the assumed geometry of the slip surface is based on observations on either small scale model tests or full scale structures. The methods vary in the geometry of the assumed failure surface, the definition of the factor of safety and the forces assumed to act on the active zone. Patra and Basudhar (2001) presented an overview of experimental and theoretical studies leading to the development of various methods of analysis of soil nailed structures.

The methods proposed by Ramlingaraju (1996) and Gupta (2003) are based on moment equilibrium approach assuming the rupture surface as log-spiral meeting the ground at 90°. The formation of log-spiral rupture surface is supported by earlier investigators (Jewell, 1989; Plumelle and

* Emeritus Fellow, Department of Civil Engineering, IIT, Roorkee – 247667, India.

† Asst. Professor, Department of Civil Engineering, IIT, Roorkee – 247667, India.

‡ Research Scholar, Department of Civil Engineering, IIT, Roorkee – 247667, India.

Schlosser, 1990; Juran and Elias, 1990; Bridle and Barr, 1990) including the observations of Ramlingaraju (1996) in his small scale model tests and trench tests. Chen (1975) showed that log-spiral mechanism is kinematically most admissible because soil particles on the slip surface move outward from the stable zone and not into it as the unstable soil wedge moves.

The behaviour of soil nailed walls under dynamic loads have been studied by very few investigators. Mizuno and Chen (1984) performed seismic analysis of vertical slopes using plasticity models and compared the results between the finite element method and the limit analysis method. Sabahit et al. (1996) presented a seismic design of nailed slopes based on pseudo-dynamic approach.

Saha et al. (2002) carried out dynamic analysis of soil nailed vertical cuts using an explicit finite difference tool FLAC (Fast Lagrangian Analysis of Continua) considering sinusoidal harmonic horizontal shear loading only. In this paper a pseudo-static analysis for analyzing the stability of vertical nailed excavations is presented.

Analysis

The analysis is based on the following assumptions:

(i) In the analysis, excavations are considered in cohesionless soil i.e. sands.

(ii) The failure is along a surface defined by the arc of a logarithmic spiral passing through the toe and intersecting the ground at right angle. The center of the spiral is located on a straight line which rises at an angle ϕ to the horizontal and passes through the point where the failure surface meets the ground as shown in Fig.1.

(iii) The deformations of the soil in the active zone are sufficient to fully mobilize the shear strength of the soil over the entire failure surface

(iv) The shear resistance of the nail due to nail bending stiffness is determined by using the plastic analysis method suggested by Jewell and Pedley (1990). The shear resistance mobilized in the nail is calculated by limiting the soil bearing pressure to the safe value given by Eqn.1.

$$\sigma_b = \sigma_v \left(\frac{1+K_A}{2}\right)\tan\left(\frac{\pi}{2}+\frac{\phi}{4}\right)e^{\left(\frac{\pi}{2}+\phi\right)\tan\phi} \tag{1}$$

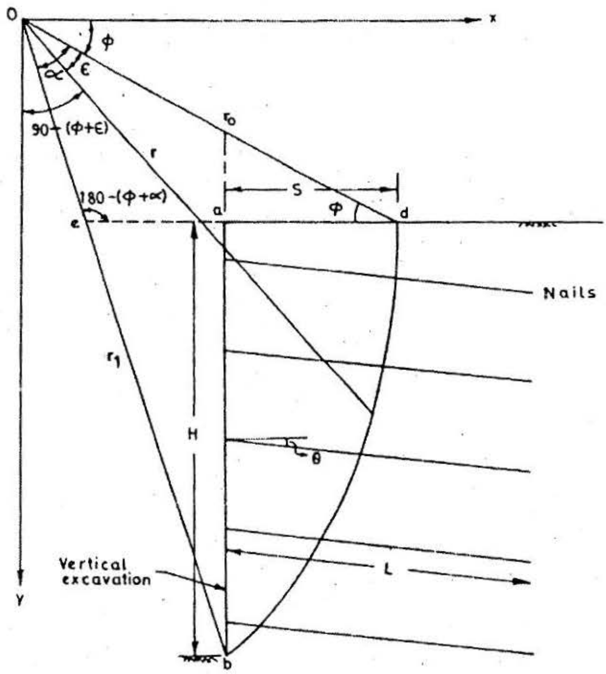

FIGURE 1 : Geometry of the Rupture Surface

where σ_b = Limit bearing stress between the soil and nail

σ_v = Vertical stress

ϕ = Angle of internal friction of soil

K_A = Coefficient of active earth pressure.

(v) The stress on the nail along its axis is assumed to be K_A times the normal stress.

(vi) The internal failure mode of the wall is either by pull-out or rupture or excessive bending leading to the formation of a plastic hinge in the nail whichever is critical.

(vii) The horizontal and vertical seismic forces are taken in terms of horizontal and vertical seismic coefficients a_h and a_v.

Geometry of Rupture Surface

Figure 1 shows a vertical excavation of height H with face ab. The rupture surface is taken as log-spiral having Eq. 2.

$$r = r_o e^{\varepsilon \tan\phi} \tag{2}$$

where r_o = Initial radius of log-spiral
ε = Angle between initial radius of log-spiral r_o and any radius of log-spiral r
r = Radius of log-spiral at an angle ε measured from initial radius

The log-spiral is intersecting the ground at 90° at a distance of S from point 'a'. The center of log-spiral lies on the line *od* making angle ϕ with horizontal. α is the angle of log-spiral (i.e. angle bod).

Considering Δoed:

$$\frac{oe}{\sin\phi} = \frac{de}{\sin\alpha} = \frac{r_o}{\sin(\phi+\alpha)} \tag{3}$$

From Δeba:

$$ea = H\cot(\phi+\alpha) \tag{4}$$

$$eb = H\,\text{cosec}(\phi+\alpha) \tag{5}$$

From log-spiral property

$$r_1 = ob = (oe + eb) = r_o\, e^{\alpha\tan\phi} \tag{6}$$

Putting the values of *oe* and *eb* from Eqns.3 and 5 in Eqn.6, we get

$$\frac{r_o \sin\phi}{\sin(\phi+\alpha)} + H\,\text{cosec}(\phi+\alpha) = r_o\, e^{\alpha\tan\phi}$$

or

$$r_o = \frac{H\,\text{cosec}(\phi+\alpha)}{e^{\alpha\tan\phi} - \dfrac{\sin\phi}{\sin(\phi+\alpha)}} = H\cdot x \tag{7}$$

where
$$x = \frac{\text{cosec}(\phi+\alpha)}{e^{\alpha\tan\phi} - \dfrac{\sin\phi}{\sin(\phi+\alpha)}} \tag{8}$$

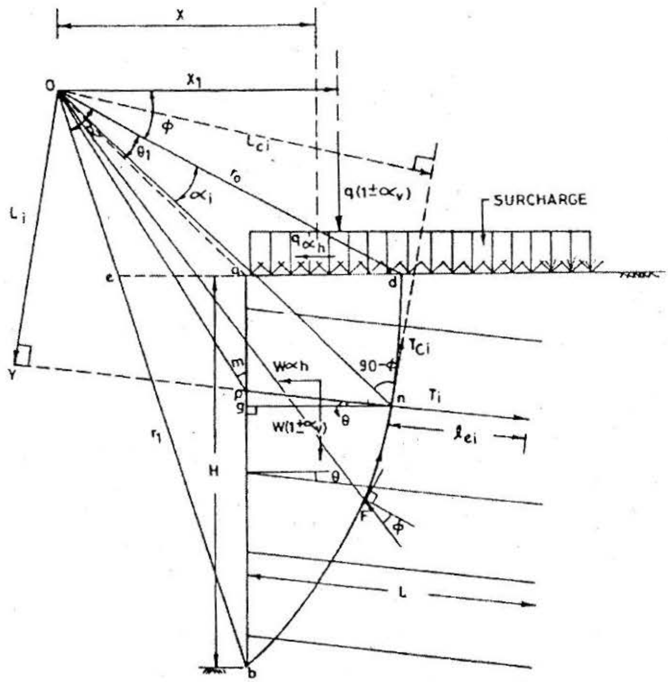

FIGURE 2 : Forces Acting on the Wedge '*abd*'

$$ad = S = de - ae = \frac{H \cdot x \cdot \sin\alpha}{\sin(\phi-\alpha)} - H\cot(\phi+\alpha) = H \cdot y \tag{9}$$

where
$$y = \frac{x \cdot \sin\alpha}{\sin(\phi-\alpha)} - \cot(\phi+\alpha) \tag{10}$$

Forces Acting on the Wedge

The forces acting on the sliding wedge are shown in Fig.2. These are described as below:

Weight W of the wedge 'abd' alongwith vertical seismic force i.e. $W(1\pm\alpha_v)$

W = Weight of '*obd*' − Weight of '*oed*' − Weight of '*aeb*'

Moment M_1 of weight W_1 of '*obd*' about O (Fig.3) is given by:

$$M_1 = \int_0^{\alpha} \gamma \cdot \frac{1}{2} r \cdot r\, d\varepsilon \cdot \frac{2}{3} r\cos(\varepsilon+\phi)$$

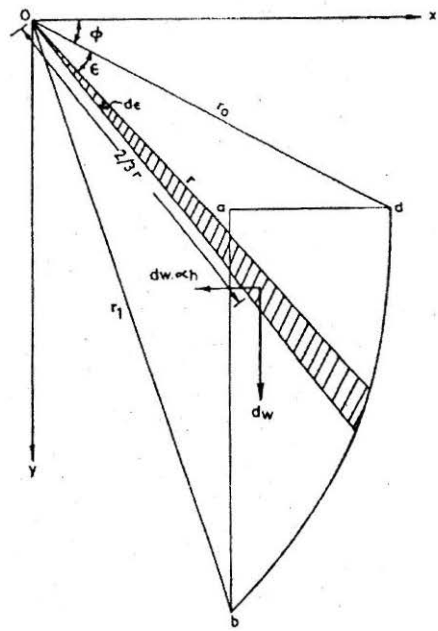

FIGURE 3 : Illustrating the Procedure for Getting Moment of Weight and Inertia Force of Wedge '*abd*'

or

$$M_1 = \frac{\gamma H^3 x^3}{3\left(1+9\tan^2\phi\right)}\left[e^{3\alpha\tan\phi}\begin{Bmatrix}3\tan\phi\cdot\cos(\alpha+\phi)\\+\sin(\alpha+\phi)\end{Bmatrix}-4\sin\phi\right] \tag{11}$$

Now, moment M_2 of weight W_2 of '*oed*' about O (Fig.4) shall be determined as below:

By geometry of the figure,

$$\delta = \cot^{-1}\left[\frac{1}{\sin\phi}\left\{\frac{2\sin(\phi+\alpha)}{\sin\alpha}-\cos\phi\right\}\right] \tag{12}$$

Therefore,

$$M_2 = \frac{1}{12}\gamma H^3\cdot x^3\cdot\frac{\sin^3\alpha}{\sin^3(\phi+\alpha)}\cdot\frac{\sin(\phi+\delta)\cdot\sin^2\phi\cdot\cos(\phi+\delta)}{\sin^2\delta} \tag{13}$$

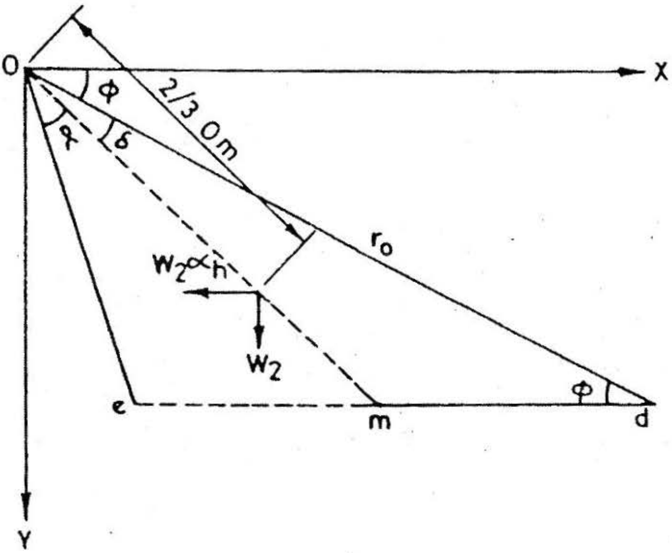

FIGURE 4 : Illustrating the Procedure for Getting Moment of Weight and Inertia Force of Wedge '*oed*'

Similarly, moment M_3 of Weight W_3 of '*aeb*' about O (Fig.2) is given by

$$M_3 = \frac{1}{2}\gamma H^3 \cot(\phi+\alpha)\left[x\cos\phi - y - \frac{\cot(\phi+\alpha)}{3}\right] \tag{14}$$

For pseudo-static analysis, the moment of vertical component of weight of wedge (*abd*) about O shall be:

$$M_{WV} = (1 \pm \alpha_v)\left[M_1 - M_2 - M_3\right] \tag{15}$$

Moment of $W \cdot \alpha_h$ *about O*

Moment M_4 of $W_1 \cdot \alpha_h$ about O (Fig.3)

$$M_4 = \int_o^{\alpha} \gamma \cdot \frac{1}{2} \cdot r \cdot r \cdot d\varepsilon \cdot \frac{2}{3} \cdot r \sin(\varepsilon+\phi) \cdot \alpha_h$$

or

$$M_4 = \frac{\gamma H^3 x^3 \cdot \alpha_h}{3(1+9\tan^2\phi)}\begin{bmatrix} e^{3\alpha\tan\phi}\left\{3\tan\phi\cdot\sin(\phi+\alpha) - \cos(\phi+\alpha)\right\} \\ -3\tan\phi\cdot\sin\phi + \cos\phi \end{bmatrix} \tag{16}$$

Similarly, moment M_5 of $W_2 \cdot \alpha_h$ about 'O' (Fig.4)

$$M_5 = \frac{1}{12}\gamma H^3 \cdot \alpha_h \cdot x^3 \frac{\sin^3 \alpha}{\sin^3(\phi+\alpha)} \cdot \frac{\sin^2(\phi+\delta)\cdot \sin^2 \phi}{\sin^2 \delta} \tag{17}$$

and, moment M_6 of $W_3 \cdot \alpha_h$ about 'O'

$$M_6 = \frac{1}{2}\gamma H^3 \cdot \alpha_h \cot(\phi+\alpha)\left[x \sin\phi + \frac{1}{3}\right] \tag{18}$$

Therefore Moment of horizontal component of weight of wedge (*abd*) alongwith horizontal seismic coefficient about 'O' shall be

$$M_{WH} = \left[M_4 - M_5 - M_6\right] \tag{19}$$

Moment of $q(1 \pm \alpha_v)$ about 'O'

$$M_{qv} = q \cdot H^2 \cdot y\left[x\cos\phi - \frac{y}{2}\right]\cdot(1 \pm \alpha_v) \tag{20}$$

Moment of $q \cdot \alpha_h$ about 'O'

$$M_{qh} = q \cdot H^2 \cdot \alpha_h \cdot x \cdot y \cdot \sin\phi \tag{21}$$

Moment of resultant frictional force 'F'

According to the property of log-spiral, in cohesionless soils, the resultant frictional force will pass through the centre of the log-spiral. Therefore its moment will be zero.

Moment due to pull out resistance of the length of nails behind the slip surface

From Fig.2,

$$l_{ei} = L - pn \tag{22}$$

$$L_i = on \sin(\phi + \alpha_i - \theta) \tag{23}$$

where α_i is the angle between (d, O) and intersection of i[th] nail with failure wedge.

$$L_{ci} = on\cos\phi \tag{24}$$

$$M_{Ti} = \sum T_i L_i \tag{25}$$

where $$T_i = \left(c + \sigma_{ni}\tan\delta\right) p_i\, l_{ci} / S_h \tag{26}$$

Also

$$T_i = f_y \cdot A / S_h \tag{27}$$

The value of T_i is chosen from Eqn.26 or 27 whichever gives the lower value.

where
f_y = Yield strength of nail
A = Cross section area of the nail = $\frac{\pi}{4}d^2$
d = Diameter of nail
c = Unit cohesion of the soil (in the present case $c = 0$).
δ = Mobilised soil-nail interface friction angle
p_i = Perimeter of the ith nail
l_{ei} = Length of the ith nail behind the failure surface
θ = Nail inclination with horizontal (degrees)
s_{ni} = Normal stress at the mid depth of ith nail in the length l_{ei}.

$$= \frac{\left(\sigma_y\cos^2\theta - \sigma_x\sin^2\theta\right)}{\left(\cos 2\theta + \sin 2\theta\tan\delta\right)} \tag{28}$$

$$\sigma_x = K_A \cdot \sigma_y \tag{29}$$

$$\sigma_y = \left\{\gamma\left(i - \tfrac{1}{2}\right)S_v + q\right\} \tag{30}$$

$$K_A = \frac{1-\sin\phi}{1+\sin\phi} \tag{31}$$

Moment of the mobilized shear acting in the nails normal to their axis

$$M_{Tci} = \sum T_{ci} L_{ci} \tag{32}$$

where T_{ci} = Mobilised shear in i[th] nail. It acts normal to the nail axis.

According to Jewell and Pedley (1990)

$$T_{ci} = \frac{C\,M_p}{l_{si}\,S_h}\left[1-\left(\frac{T_i}{T_p}\right)\right] \tag{33}$$

where C = a constant and is equal to 4 for plastic analysis

l_{si} = Shear width

$$= \sqrt{\frac{8\,M_p}{\sigma_b \cdot d}\cdot\left(1-\frac{T_i}{T_p}\right)} \tag{34}$$

(If grouted nails are used, then, d is replaced by D, where D = Grout hole diameter)

T_i = Axial force in the i[th] nail at the point of maximum bending moment (Eqns.26 and 27)

T_p = Fully plastic axial force

$= f_y \times A$

$$\sigma_b = \sigma_v\left(\frac{1+K_A}{2}\right)\tan\left(\frac{\pi}{4}+\frac{\phi}{2}\right)e^{\left(\pi/2+\phi\right)\tan\phi} \tag{35}$$

σ_v = $\gamma \times$ Depth of nail from top

K_A = Coefficient of active earth pressure (Eqn.31)

M_p = Fully plastic moment capacity of nail

The value of M_p depends on the nail yield strength and shape of the nail. For various shapes of the nail, the values of M_p are listed in Table 1.

The equation of factor of safety will be given by:

$$\text{F.O.S.} = \frac{\sum T_i\,L_i + \sum T_{ci}\,L_{ei}}{M_{WV} + M_{WH} + M_{qV} + M_{qH}} \tag{36}$$

TABLE 1 : Values of M_p Corresponding to Nail Section

Shape of Nails	Value of M_p
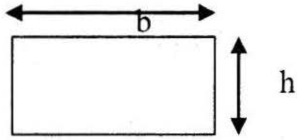	$\frac{bh^2}{4} f_y$
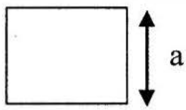	$\frac{a^3}{4} f_y$
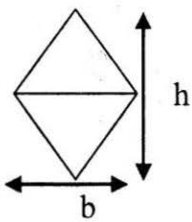	$\frac{bh^2}{12} f_y$
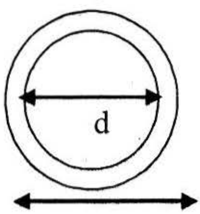	$\frac{1}{6}\left(D^3 - d^3\right) f_y$
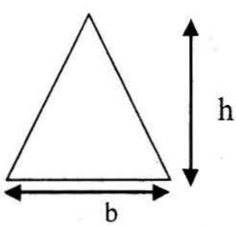	$0.0976\, b h^2 f_y$
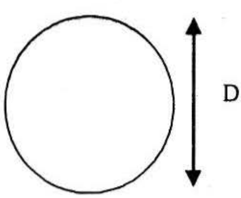	$0.166\, D^3 f_y$

Parametric Study

The factor of safety (Eqn.36) was obtained for the following parameters

Height of excavation	: 4.0 m, 6.0 m, 8.0 m, 10.0 m
Soil type	: Cohesionless soil (i.e. $c = 0$)
Angle of internal friction, ϕ	: 25°, 30°, 35°
Length of nail-height of excavation ratio (L/H)	: 0.6, 0.7, 0.8
Surcharge on nailed wall (q)	: 0.0 kN/m^2, 80 kN/m^2
Diameter of the nail	: 25 mm
Type of the nail	: Driven
Nail inclination, θ	: 0°
Yield strength of nail (f_y)	: 250×10^6 N/m^2
Soil-nail interface friction angle (δ)	: $2/3\phi$

The horizontal spacing of the nails (S_h) is considered equal to vertical spacing (S_v). The vertical spacing (S_v) has been chosen so that factor of safety works out approximately between 1.0 to 2.0.

For the given combination of parameters of soil nailed wall, the factor of safety (F.O.S.) was computed for various values of log-spiral angle α. A typical plot between F.O.S. and angle α is shown in Fig.5. From such plots, minimum values of F.O.S. were obtained, and the same are given in Tables A1 to A6 of Appendix-A for few cases.

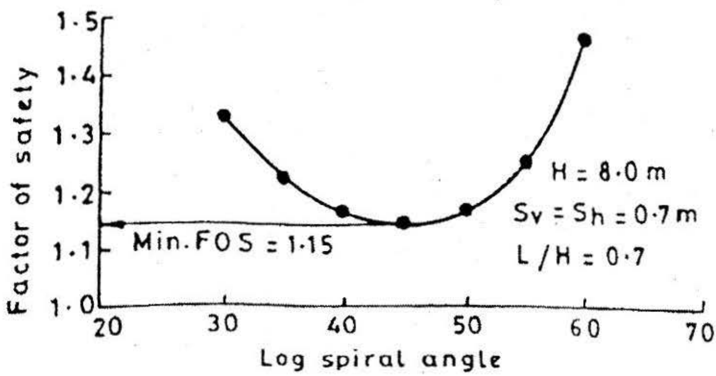

FIGURE 5 : F.O.S. Vs. Log-Spiral Angle α

Before preparing these tables, some typical cases were analysed. These typical cases helped in giving the reasoning of selecting the parameters for preparing the tables, and also suggesting modification in using F.O.S. values specifically with respect to nail diameter other than 25 mm. These typical cases are discussed below:

(i) Firstly a study was carried out considering the variation of nail inclination with horizontal (θ). Typical results are given below in Table 2.

It is evident from this table that the factor of safety (F.O.S.) is maximum for $\theta = 0°$ i.e. using horizontal nails in excavations having vertical face. Similar trend was observed in other combinations of parameters. Keeping this fact in view the results are presented only for $\theta = 0°$ case. Earlier investigators (Juran and Elias, 1990; Sabahit et al., 1996; Patra, 1998 and Patra et al., 2001) have also obtained similar results.

(ii) Table 3 summarizes the typical results considering variation in diameter of nails. It can be observed from this table that the F.O.S. increases approximately in direct proportion to the increase in diameter of nail. The maximum difference was observed as 9.7% only. The Tables A1 to A6 are prepared taking 25 mm as the diameter of the nail. For other diameter of nails (x mm), the results presented in Tables A1 to A6 may be used by multiplying them with $x/25$.

(iii) Table 4 has been prepared showing values of F.O.S. for two different values of nail yield stress (f_y) as 250×10^6 N/m^2 and 415×10^6 N/m^2. Typical computations have been done for different values of H, S_v, α_h and α_v.

TABLE 2 : Variation of F.O.S. with Nail Inclination θ
(H = 8.0 m, $S_v = S_h$ = 0.4 m, ϕ = 30°, $\alpha_h = \alpha_v$ = 0, L/H = 0.7)

Nail Inclination with Horizontal, θ (deg.)	Minimum Value of Factor of Safety
0	2.905
5	2.776
10	2.639
15	2.484
20	2.321
25	2.143

TABLE 3 : Variation of F.O.S. with Nail Diameter (H = 6.0 m, L/H = 0.6, ϕ = 35°, q = 80 kPa)

S.No.	Case Studies	F.O.S. d = 25 mm	F.O.S. d = 32 mm	F.O.S. Col. 3 × 32/25	% difference in values of Col. 4 and 5
(1)	(2)	(3)	(4)	(5)	(6)
1.	$\alpha_h = 0$				
(a)	$H = 6.0$ m, $S_v = 0.5$ m	1.351	1.868	1.729	7.44
(b)	$H = 8.0$ m, $S_v = 0.6$ m	1.220	1.667	1.561	6.36
2.	$\alpha_h = 0.1$				
(a)	$H = 6.0$ m, $S_v = 0.5$ m	1.084	1.510	1.387	8.14
(b)	$H = 8.0$ m, $S_v = 0.5$ m	1.201	1.620	1.537	5.12

The values of F.O.S. given in Columns 3 and 4 of Table 4 show that the maximum difference in the values of F.O.S. for different values of f_y is of the order of 8.9%, 7.1% and 5.9% only for L/H = 0.6, 0.7 and 0.8 respectively. Similar trend is seen in the values given in Columns 5 and 6. Tables A1 to A6 were prepared for the value of f_y equal to 415×10^6 N/m^2. In Table 4, F.O.S. values for f_y equal to 250×10^6 N/m^2 have also been given because in the field usually nails are not used having f_y value less than 250×10^6 N/m^2.

TABLE 4 : Variation of F.O.S. with f_y (ϕ = 25°)

S. No.	L/H	$H = 6$ m, $c = 0$, $q = 80$ kPa, $S_v = 0.4$, $\alpha_h = 0.05$, $\alpha_v = 0.025$		$H = 8$ m, $c = 0$, $q = 0$ kPa, $S_v = 0.35$, $\alpha_h = 0.15$, $\alpha_v = 0.075$	
		$f_y = 250 \times 10^6$ N/m^2	$f_y = 415 \times 10^6$ N/m^2	$f_y = 250 \times 10^6$ N/m^2	$f_y = 415 \times 10^6$ N/m^2
(1)	(2)	(3)	(4)	(5)	(6)
1	0.6	1.33	1.46	1.25	1.44
2	0.7	1.7	1.83	1.53	1.73
3	0.8	2.06	2.19	1.85	·2.05

TABLE 5 : Variation of F.O.S. with *L/H*

S. No.	L/H	$H = 10$ m, $c = 0$, $q = 80$ kPa, $S_v = 0.35$, $\alpha_h = 0.1$, $\alpha_v = 0.05$, $\phi = 25°$		$H = 10$ m, $c = 0$, $q = 80$ kPa, $S_v = 0.6$, $\alpha_h = 0.1$, $\alpha_v = 0.05$, $\phi = 35°$	
		FOS_{min}	% Increase	FOS_{min}	% Increase
(1)	(2)	(3)	(4)	(5)	(6)
1	0.6	1.73	–	1.16	–
2	0.7	2.23	29.29	1.50	29.49
3	0.8	2.82	63.52	1.83	57.15

(iv) The Table 5 shows the change in the values of F.O.S. with variation in L/H.

A perusal of Table 5 shows that the value of F.O.S. increases with increase in L/H ratio. The F.O.S. increases by about 30% when L/H increases from 0.6 to 0.7 and it increases to about 60% when the L/H increases from 0.6 to 0.8.

A critical examination of Tables A1 to A6 shows that for other parameters keeping same, the factor of safety increases with the increase in the height of excavation. It is due to the fact that nails located at deeper depths provide higher resistance.

Illustrative Example

Design a vertical faced nailed wall of height 8.0 m carrying a surcharge of 80 kN/m^2 on it. The soil material is cohesionless with $\phi = 30°$. The wall is located in a seismic region having the value of horizontal seismic coefficient as 0.10.

Solution

(i) Considering $\alpha_h = 0.1$

Adopt $L/H = 0.6$, d = 25 mm, Yield Strength, $f_y = 415 \times 10^6$ N/m^2

From Table A5,

For $\phi = 30°$, $\alpha_h = 0.1$, $H = 8.0$ m, $L/H = 0.6$,

For $S_v = 0.35$ m, F.O.S. = 1.79

For S_v = 0.40 m, F.O.S. = 1.30

Linear interpolation gives S_v = 0.38 m for F.O.S. = 1.50

(ii) Considering α_h = 0.0

For S_v = 0.4 m, F.O.S. = 1.64

For S_v = 0.45 m, F.O.S. = 1.33

Linear interpolation gives S_v = 0.42 m for F.O.S. = 1.50

It is clear from this example that a vertical excavation can be stabilized by soil-nailing technique providing the nails at spacing of 0.38 m in a seismic region having α_h = 0.1. In non-seismic region (i.e. α_h = 0), the spacing between nails can be increased to 0.42 m to give the same factor of safety i.e. 1.5.

Conclusions

1. In vertical excavations, maximum factor of safety is obtained when horizontal nails are used i.e. inclination of nail with horizontal is zero.

2. The factor of safety increases approximately in direct proportion with the increase in diameter of nail.

3. The factor of safety increases marginally with the increase in the yield strength of nail.

4. Factor of safety increases appreciably with increase in L/H from 0.6 H to 0.8 H.

5. The factor of safety increases significantly with the increase in height of excavation.

References

BRIDLE, R.J. and BARR, B.I.G. (1990), "The Analysis and Design of Soil Nails", Performance of Reinforced Soil Structures, *Proc. of Int. Reinforced Soil Conf.*, Glasgow, pp.249-254.

CHEN, W.F. (1975), "Limit Analysis and Soil Plasticity", *Developments in Geotech. Engg.*, Vol. 7, Elsevier Scientific Publishing Company.

ELIAS, V. and JURAN, I. (1989), "Manual of Practice for Soil Nailing", *Federal Highway Administration Report FHWA/RD-89/198.*

GUPTA, R.P. (2003), "A Study on Soil Nailing with Respect to Open Excavations and Slopes", *M.E. Thesis*, Indian Institute of Technology, Roorkee.

JEWELL, R.A. (1989), "Theory of Reinforced Walls : Revised Design Charts for Steep Reinforced Slopes", *Proc. of the Conf. on Reinforced Embankments, Theory and Practice in the British Isles*, Cambridge University, pp.1-30.

JEWELL, R.A. and PEDLEY, M.J. (1990), "Analysis for Soil Reinforcement with Bending Stiffness", *ASCE J. Geotech Engg.*, Vol.118, No.10 pp.1505-1528.

JURAN, I. and ELIAS, V. (1990), "Behaviour and Working Stress Design of Soil Nailed Retaining Structures", Performance of Reinforced Soil Structures, *Proc. of Int. Reinforced Soil Conf.*, Glasgow, pp.207-212.

MIZUNO, E. and CHEN, W.F. (1984), "Plasticity Models for Seismic Analysis of Slopes", *Int. Journal of Soil Dynamics and Earthquake Engineering*, pp.2-7.

PATRA, C.R. (1998), "Sequential Minimization Technique in the Optimum Design of Slopes with or without Nails", *Ph.D. Thesis*, IIT Kanpur.

PATRA, C.R. and BASUDHAR, P.K. (2001), "Nailed Soil Structure : An Overview", *Indian Geotechnical Journal*, Vol.31, No.4, pp.322-362.

PLUMELLE, C. and SCHLOSSER, F. (1990), "A French National Research Project on Soil Nailing: Clouterre", Performance of Reinforced Soil Structure, *Proc. of Int. Reinforced Soil Conf.*, Glasgow, pp.219-223.

RAMALINGARAJU, G.V. (1996), "Behaviour of Nailed Soil Retaining Structures", *Ph.D. Thesis*, Nanyang Technical University, Singapore.

SABAHIT, N., MADHAV, M.R. and BASUDHAR, P.K. (1996), "Seismic Analysis of Nailed Soil Slopes", *Proc. IS Kyushu Int. Symp. on Earth Reinforcement*, Kyushu, Japan, pp.347-352.

SAHA, N., MURTHY, B.R.S. and VATSALA (2002), "Soil Nailed Walls under Dynamic Loads", *12th Symp. on Earthquake Engineering*, IIT Roorkee, pp.434-441.

SCHLOSSER, F. (1982), "Behaviour and Design of Soil Nailing", *Symposium on Recent Developments in Ground Improvement Techniques*, Bangkok, pp.399-413.

SHEN, C.K., BANG, S., ROMSTAD, K.M., KULCHIN, L. and DENATALE, J.S. (1981), "Field Measurements of an Earth Support System", *ASCE J. Geotech. Engg.*, Vol.107, No.GT12, pp.1625-1642.

STOCKER, M.F., KORBER, G.W., GASSLER, G. and GUDEHUS, G. (1979), "Soil Nailing", *C.R. Coll. Int. Reinforcement Des Sols*, Paris, pp.469-474.